

Eyes Will Shut: A Vision-Based Next GPS Location Prediction Model by Reinforcement Learning from Visual Map Feed Back

Ruixing Zhang¹, Yang Zhang¹, Tongyu Zhu^{1,2}, Leilei Sun^{1,2}, Weifeng Lv^{1,2}

¹ the State Key Laboratory of Complex and Critical Software Environment, Beihang University

²H3I, Beihang University

³China Mobile Information Technology Center

yyxzhj@buaa.edu.cn, yannazhang@buaa.edu.cn, leileisun@buaa.edu.cn, tongyuzhu@buaa.edu.cn, lwf@buaa.edu.cn

Abstract

Next Location Prediction is a fundamental task in the study of human mobility, with wide-ranging applications in transportation planning, urban governance, and epidemic forecasting. In practice, when humans attempt to predict the next location in a trajectory, they often visualize the trajectory on a map and reason based on road connectivity and movement trends. However, the vast majority of existing next-location prediction models do not reason over maps **in the way that humans do**. Fortunately, the recent development of Vision-Language Models (VLMs) has demonstrated strong capabilities in visual perception and even visual reasoning. This opens up a new possibility: by rendering both the road network and trajectory onto an image and leveraging the reasoning abilities of VLMs, we can enable models to perform trajectory inference in a human-like manner. To explore this idea, we first propose a method called Vision-Guided Location Search (VGLS), which evaluates whether a general-purpose VLM is capable of trajectory-based reasoning without modifying any of its internal parameters. Based on insights from the VGLS results, we further propose our main approach: VLMLocPredictor, which is composed of two stages: In the first stage, we design two Supervised Fine-Tuning (SFT) tasks that help the VLM understand road network and trajectory structures and acquire basic reasoning ability on such visual inputs. In the second stage, we introduce Reinforcement Learning from Visual Map Feedback, enabling the model to self-improve its next-location prediction ability through interaction with the environment. Experiments conducted on datasets from four different cities show that our method achieves state-of-the-art (SOTA) performance and exhibits superior cross-city generalization compared to other LLM-based approaches. Case studies further demonstrate that, through our framework, VLMs learn to reason effectively over road networks, substantially enhancing their next-location prediction capabilities. The code is <https://github.com/Rising0321/VLMLocPredictor>.

Introduction

With the proliferation of smartphones and various IoT devices, vast amounts of GPS location data have been collected in recent years, ranging from individual signaling data to vehicle trajectories. To fully unlock the value of this data, next GPS location prediction has become a critical task in spatial-temporal analysis, with broad applications in traffic resource allocation(Zhang et al. 2025a; Fang et al. 2019;

Zhang and Patras 2018), epidemic spread forecasting(Zhang et al. 2025b; Zhao et al. 2024; Mayemba et al. 2024), and urban governance(Cabanas-Tirapu et al. 2023; Wang et al. 2019; Pappalardo et al. 2019).

Traditionally, this task has been approached through sequence modeling techniques. In early studies, researchers modeled population movement using Markov chains(Gao et al. 2019), relying on first-order dependencies to predict the next location point. With the emergence of the Recurrent Neural Network and Transformer, models like DeepMove(Feng et al. 2018) enabled learning richer representations by compressing long-range historical information, significantly improving prediction accuracy. Then, researchers recognized the importance of spatial topology, leading to the incorporation of graph neural networks that model road network structures(Long, Yuan, and Li 2025; Yang, Liu, and Zhao 2022). With the rise of Large Language Models (LLMs) the researchers have utilized LLMs to using the rich semantic information to aid next location prediction(Feng et al. 2025; Liu et al. 2024).

However, most of these methods depart from how humans reason about movement. When predicting the next location, humans typically visualize trajectories over a map and reason jointly based on trajectory trends, road network connectivity, and natural assumptions (e.g., shortest paths, flow direction). Current models, in contrast, lack this form of map-based visual reasoning.

Fortunately, the emergence of Vision-Language Models (VLMs) has demonstrated strong capabilities in visual understanding and multimodal reasoning. This motivates our central hypothesis: **Can we enable VLMs to reason over visualized maps and trajectories, thereby mimicking human-like trajectory inference for next-GPS-location prediction?**

To test this, we first propose a diagnostic framework, Vision-Guided Location Search (VGLS), which evaluates whether a pretrained VLM possesses any innate trajectory reasoning ability, without modifying its internal parameters. Our preliminary experiments show that larger VLMs exhibit some capacity for trajectory reasoning, while smaller VLMs perform near-random, indicating a significant capability gap.

Therefore, transferring VLMs to next-GPS-location prediction is thus non-trivial, and presents two key challenges:

- **How can we improve a VLM’s ability to reason over visual trajectories in an autonomous way?** Inspired by the success of Reinforcement Learning with Verifiable Reward (RLVR) in models like GPT-o1 (OpenAI 2024c) and DeepSeek-R1 (Guo et al. 2025), we explore RLVR as a scalable post-training paradigm. However, applying RL to visual trajectory prediction presents new difficulties. Therefore, designing task-aligned reward functions and interactive environments that can encourage the model to learn visual-spatial reasoning remains an open problem.
- **How can we endow trajectory reasoning abilities to models that lack them?** As shown in our VGLS results, many models exhibit almost no ability to reason over visual maps. Yet reinforcement learning often yields unexplainable results unless the model possesses minimal domain-specific priors. Moreover, most models lack the ability to localize trajectory points precisely on the image, making visual reasoning brittle. This calls for a structured approach to progressively instill fine-grained visual grounding and reasoning capabilities.

To address these challenges, we propose VMLocPredictor, the first framework to enable VLM-based next-GPS-location prediction using a combination of supervised fine-tuning and reinforcement learning over visual maps. First, we introduce a two-stage supervised fine-tuning (SFT) process: In Stage 1, we fine-tune the model using a coordinate annotation task, where the VLM learns to locate trajectory points on the visual map, thus acquiring precise spatial grounding. In Stage 2, we combine this with chain-of-thought annotations (generated by Claude 3.5 Sonnet) to teach the model to perform basic visual trajectory reasoning, without forgetting coordinate understanding. Next, we propose Reinforcement Learning from Visual Map Feedback. We design a GRPO-based RL framework tailored for visual reasoning, with two key reward functions: Distance Reward and Road Reward. By fine-tuning a Qwen2-VL model using this two-stage SFT + RL pipeline, we obtain VMLocPredictor. Experiments on datasets from four cities show that our method achieves state-of-the-art performance and demonstrates significantly better cross-city generalization than existing LLM-based approaches.

Our main contributions are summarized as follows:

- We propose the first VLM-based framework for next-GPS-location prediction. Our key insight is that when trajectory and map information are fused into a single image, the VLM can treat this as a visual reasoning problem, enabling human-like generalization across cities.
- We design a reinforcement learning post-training framework to improve VLMs’ visual trajectory reasoning ability. Our approach enables models to self-improve through interaction with map-based environments. Additionally, we introduce Vision-Guided Location Search (VGLS) as a plug-and-play tool to assess next-point reasoning ability without fine-tuning.
- Our method achieves SOTA results on all benchmarks and significantly outperforms other LLM-based approaches in terms of cross-city transferability. Case studies further show that our model learns to reason effec-

tively over road networks, similar to human navigation behavior.

Preliminaries

Definitions

Definition 1 (Trajectory): Let a trajectory \mathbf{T} be defined as an ordered sequence of 13 spatial points, denoted as $\mathbf{T} = \{p_1, p_2, \dots, p_{13}\}$. Each point p_i ($i = 1, 2, \dots, 13$) is represented by its geographic coordinates $p_i = (lat_i, lon_i)$, where lat_i and lon_i correspond to the latitude and longitude values, respectively. To ensure consistency and applicability in next location prediction tasks, the trajectory is processed to be uniform with a constant temporal interval $\Delta t = 45s$.

Definition 2 (Next Location Prediction): Next Location Prediction is to learn a predictive function f such that: $f(\mathbf{T}_{1:12}) = \hat{p}_{13}$, where \hat{p}_{13} is the predicted location that approximates the ground-truth p_{13} .

Group Relative Policy Optimization (GRPO)

Group Relative Policy Optimization (GRPO) is a reinforcement learning algorithm tailored for optimizing large models without relying on learned value functions (Shao et al. 2024). Instead of computing absolute advantages, GRPO evaluates the relative quality of candidate responses sampled from the same query, enabling stable learning with minimal supervision. Given an input query q , the policy π_θ generates a group of G candidate responses $\{o_1, o_2, \dots, o_G\}$, each assigned a verifiable reward $r_i = R(q, o_i) \in [0, 1]$. GRPO computes a normalized, group-relative advantage:

$$A_i = \frac{r_i - \text{mean}(r_1, \dots, r_G)}{\text{std}(r_1, \dots, r_G)}. \quad (1)$$

These scores reflect how each response compares to others within the same group. The policy is then updated by maximizing the likelihood of better responses while applying a KL penalty to maintain closeness to a reference model π_{ref} :

$$\mathcal{L}_{\text{GRPO}} = - \sum_{i=1}^G [\log \pi_\theta(o_i|q) \cdot A_i] + \beta \cdot \text{KL}(\pi_\theta(\cdot|q) \parallel \pi_{\text{ref}}(\cdot|q)). \quad (2)$$

This unified objective integrates the relative ranking signal from group-wise rewards (via A_i), and the stability constraint from the KL-regularized framework. Therefore, it allows the model to improve via verifiable feedback while maintaining response diversity and alignment with prior knowledge.

Preliminary Task: Can General VLMs make next-GPS-location prediction?

Visual Guided Location Search (VGLS)

Before delving into the core of this work, we first conduct a preliminary experiment to investigate whether general VLMs are capable of next-GPS-location prediction. If a VLM inherently possesses the ability to predict the next location point to some extent, it can be regarded as the backbone next-location prediction model. However, evaluating

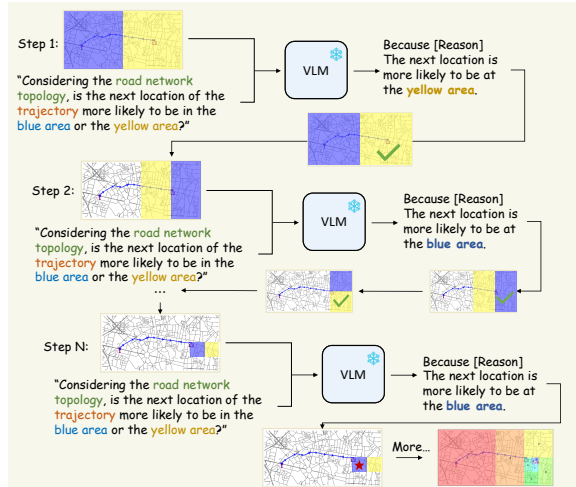


Figure 1: **An illustration of VGLS.** The image was initially divided into two halves, colored blue and yellow. After querying the VLM, the feedback was used to identify a probable region, which was then further divided, with one half colored blue and the other yellow. This refined image was reintroduced to the VLM, and the process was iteratively repeated over multiple rounds. Through this iterative feedback loop, the VLM eventually provided a feasible solution for the next location point.

whether a VLM has such generalizable predictive capabilities is non-trivial. This difficulty arises because most existing VLMs lack the ability to explicitly pinpoint coordinates on a map. Consequently, designing a method that can assess a VLM’s next-location prediction ability presents a significant challenge. Besides, given the goal of this study is to assess the visual intelligence of general VLMs, we deliberately avoid fine-tuning or task-specific adaptation methods, as such approaches would contradict the premise of evaluating general capabilities.

We are inspired from related works that proved VLMs are capable of interpreting specific regions delineated by a circle (Shtedritski, Rupprecht, and Vedaldi 2023) and can handle tasks recursively (Wu and Xie 2024). Building on these insights, we propose a Visual Guided Location Search (VGLS) mechanism. As shown in figure 1, the core idea is as follows: we begin by dividing the map into two regions, coloring one half blue and the other half yellow. The VLM is then tasked with determining whether the next trajectory point is more likely located in the blue or yellow region. Take the model identifies the blue region as more likely as an example, the blue region is further subdivided into one half colored blue and the other yellow. This iterative process is repeated for N rounds, progressively narrowing down the feasible region until a satisfactory resolution is achieved.

Fundamentally, we designed a hierarchical question-answering process. In the first iteration, the model only needs to answer a relatively simple question: which half of the map is more likely to contain the next point. As the pro-

cess continues, the questions become increasingly challenging, with scenarios emerging where both blue and yellow regions may contain plausible solutions. This iterative refinement ensures a systematic and efficient localization process, leveraging the visual reasoning capabilities of VLMs. **The approach described above enables VLMs to perform next-GPS-location prediction without modifying any of their existing parameters.**

Findings

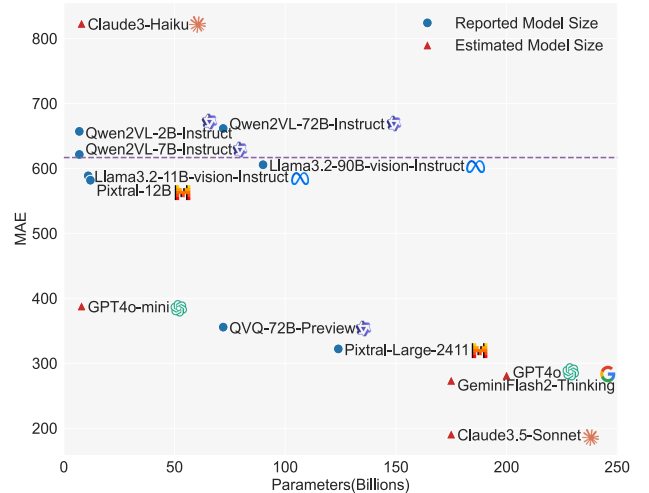


Figure 2: **The preliminary experimental results.** We observe that larger VLMs such as GPT-4o and Claude 3.5 Sonnet exhibit a certain degree of capability in next-location reasoning. In contrast, smaller VLMs such as Qwen2-VL-2B and Claude 3 Haiku currently lack this ability.

Due to space limitations, detailed experimental settings are provided in the appendix. Here, we briefly explain the key findings. As shown in Figure 2, the x-axis represents the number of model parameters, while the y-axis indicates the distance error between the predicted center point and the ground-truth next location after ten iterations. The dashed line in the figure denotes the error distribution when the model randomly outputs either yellow or blue at each iteration—representing the baseline error for a model with no ability to predict the next GPS point.

From the figure, we observe the following findings:

- Larger models such as GPT-4o, Claude 3.5, and Gemini Flash 2 exhibit a certain degree of next-location prediction capability. This suggests that some general-purpose VLMs **can** perform next-GPS-point prediction. To the best of our knowledge, this is the first work to report such a finding.
- Most smaller models, including Qwen-VL-2B and LLaVA 3.2-11B-Vision-Instruct, show performance close to random guessing, indicating a lack of effective next-point prediction ability.

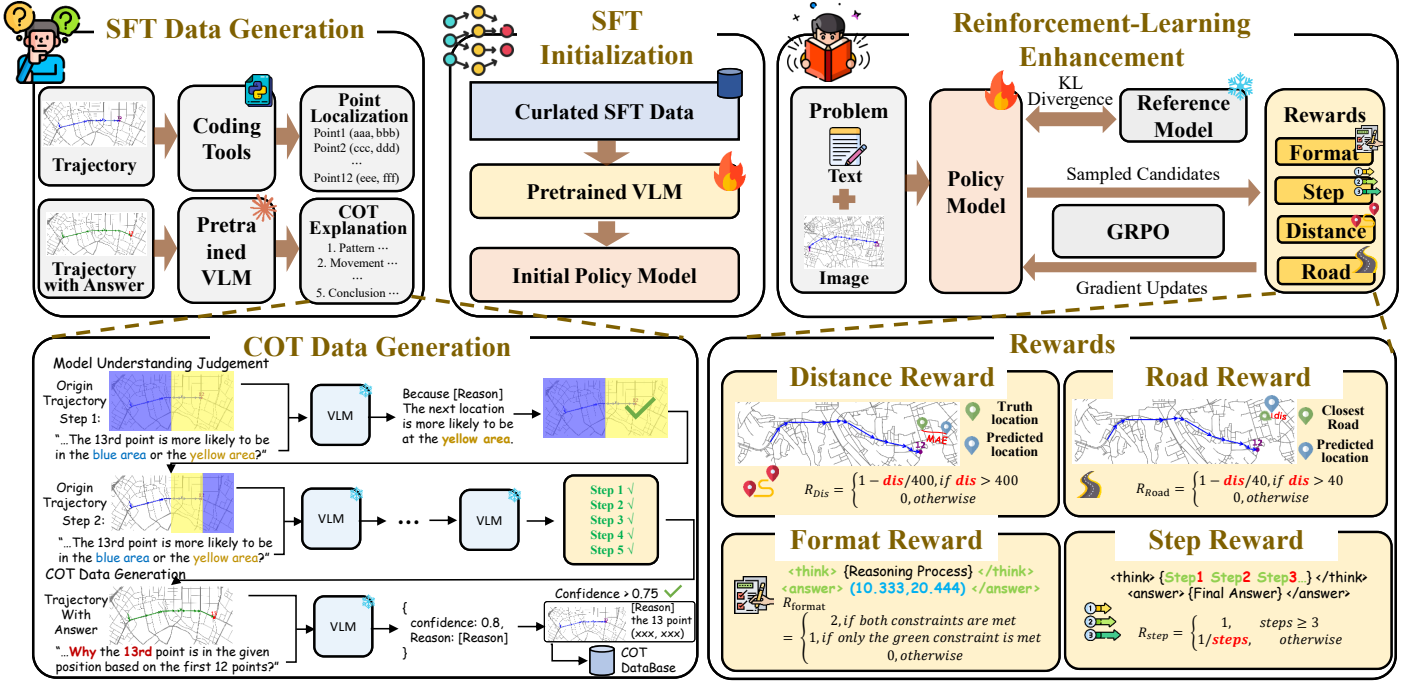


Figure 3: **The illustration of VLMLocPredictor.** Our method consists of one data generation phase and two training phases. In the data generation phase, we generate point localization data and high-quality COT data to aid the SFT phase. In the first training phase, we use a two-stage strategy to fine-tune a VLM using a carefully constructed dataset to enable it recognizing the coordinates of each point on the map and to endow it with basic trajectory reasoning skills. In the second training phase, we adopt a reinforcement learning strategy to further autonomously enhance the model’s ability.

- The ability to predict the next GPS point demonstrates a scaling law: larger models tend to make more accurate predictions.

The subsequent parts of our work are primarily built upon the first and second findings above.

VLMLocPredictor

In this section, we introduce VLMLocPredictor, a method designed to equip VLMs with next-gps-location prediction abilities through Reinforcement Learning from Visual Map Feedback. Unlike the binary classification setting in the Preliminary Task, VLMLocPredictor aims to enable the model to **directly output the coordinates of the next location point on an image**. The framework is illustrated in Figure 3. To achieve this, we design a two-stage training pipeline: 1. **SFT-based Initialization**: This stage involves supervised fine-tuning (SFT) on two tasks, aimed at teaching the VLM to mark points on a map and perform basic trajectory reasoning. 2. **RL-based Enhancement**: In this stage, we introduce four reward functions and apply GRPO-based reinforcement learning to enhance the model’s reasoning ability in predicting the next GPS point.

SFT-based Initialization

RL stage can be viewed as a means to autonomously enhance an existing capability. However, if the model lacks the

foundational ability, reinforcement learning may become extremely unexplainable. Our earlier experiments showed that some VLMs do not possess visual-based trajectory reasoning, and at the time of this submission, most VLMs cannot output precise coordinates of points on an image. Therefore, the goal of the SFT stage is to impart these two fundamental capabilities to the model. To this end, we design two supervised tasks:

Task 1: Point Localization . Given a trajectory of 12 points overlaid on a map image and one specific point, the model is required to directly output the coordinate of that point. The purpose is to ensure the model accurately understands the visual location of each point on the image. Since accurate next-gps-location prediction depends on a clear understanding of the previous points, this task serves as the foundation. The dataset used here is denoted as \mathcal{D}_1 . The construction of this dataset can be finished by common programming tools.

Task 2: COT Prediction . This task is equivalent to the main task defined in this paper: given an image showing a trajectory of 12 points, the model is required to predict the coordinates of the 13rd point. In this task, we additionally require the model to output a reasoning chain that explains how the prediction is made. This task helps the model acquire basic next-location reasoning ability, and the corre-

sponding dataset is denoted as \mathcal{D}_2 . **However, to train the model with chain-of-thought (CoT) supervision, we first need to obtain CoT data specifically tailored to the next-location prediction task.**

Based on the findings from the Preliminary Task, Claude 3.5-Sonnet demonstrated strong capabilities in visual trajectory reasoning, making it a suitable choice for generating chain-of-thought (CoT) data. To ensure the reliability of the generated CoT, we design the following three-step procedure:

- We first leverage the Vision-Guided Location Search (VGLS) method from the Preliminary Task. If a trajectory consistently yields correct predictions across the first five iterations of VGLS, we consider the model to have a strong understanding of that trajectory.
- Although Claude 3.5-Sonnet cannot directly output the coordinates of a point on the image, we provide it with the full image containing the thirteenth point and ask it to explain how the next location can be inferred from the first twelve points. Alongside the explanation, the model is also prompted to provide a confidence score for its reasoning.
- We filter and retain only those CoT outputs with a confidence score above 75%, treating them as high-quality supervision signals. By using the image with twelve trajectory points as the input and concatenating the generated CoT with the true coordinate of the thirteenth point as the output, we construct a training set for Task 2 fine-tuning.

Based on our findings from the Preliminary Task, we identify Claude 3.5 Sonnet as a model with relatively strong visual trajectory reasoning ability. Although Claude 3.5 Sonnet cannot directly output coordinate locations on the image, we provide it with trajectory images that include the 13th point, and ask it to explain how to infer the next point from the previous twelve, along with a confidence score. We retain only the explanations with a confidence score above 70% as reliable CoT samples. Then, by using the image with 12 points as input and concatenating the generated CoT reasoning with the ground-truth coordinates of the 13th point, we construct high-quality training samples for fine-tuning on Task 2.

Based on these datasets, we design a two-stage fine-tuning pipeline. In the first phase, the model is fine-tuned solely on \mathcal{D}_1 to learn accurate coordinate grounding. In the second stage, we fine-tune on both \mathcal{D}_1 and \mathcal{D}_2 to instill basic trajectory reasoning while preserving the model’s spatial understanding. This process can be formally expressed as:

$$\begin{aligned}\theta_1 &= \arg \max_{\theta \leftarrow \theta_0} \mathbb{E}_{(x,y) \sim \mathcal{D}_1} [\log p_\theta(y | x)] \\ \theta_2 &= \arg \max_{\theta \leftarrow \theta_1} \mathbb{E}_{(x,y) \sim \mathcal{D}_1 \cup \mathcal{D}_2} [\log p_\theta(y | x)]\end{aligned}\quad (3)$$

which θ denotes the parameters of the VLM, θ_0 denotes the pretrained parameters of the VLM, x represents the input (trajectory with map and prompts), y is the corresponding target output (e.g., coordinates or region choice), and $\theta \leftarrow \theta_0$ denotes the θ is initialized as θ_0 ,

RL-based Enhancement

Inspired by reinforcement learning-based post-training methods, our goal in this stage is to enhance the model’s ability to predict the next location point through reinforcement learning. Due to the high computational cost of training a value network in Proximal Policy Optimization-like frameworks, we adopt GRPO, which performs policy updates based on relative advantages within a group of sampled outputs, significantly reducing training overhead during post-training.

To guide the learning process, we design four distinct reward functions, each capturing a different aspect of desired model behavior: Distance Reward, Road Reward, Format Reward, Step Reward. We describe each of them in detail below.

Distance Reward. The most critical metric for evaluating the quality of next-gps-location prediction is the prediction error. Therefore, we directly incorporate the Euclidean distance as a reward function. Specifically, if the predicted point is more than 400 pixels away from the ground-truth location, the reward is set to 0. Otherwise, the reward is calculated as $R_{\text{dis}} = 1 - \frac{\text{dis}}{400}$. This design reflects the intuition that predictions with large errors are essentially unusable and should not be rewarded, while more accurate predictions are increasingly incentivized. The Distance reward can be formalized as:

$$R_{\text{dis}} = \begin{cases} 1 - \frac{\text{dis}}{400}, & \text{if } \text{dis} \leq 400 \\ 0, & \text{otherwise} \end{cases} \quad (4)$$

Road Reward. Since all the trajectories in our dataset lie on roads, ensuring that the predicted point also falls on the road network is crucial for usability. We find that prompting alone is insufficient to guarantee this behavior in VLMs. Hence, we introduce a Road Reward to encourage on-road predictions. The reward is calculated based on the Euclidean distance dis from the predicted point to the nearest road. If this distance exceeds 40 pixels, the reward is 0. Otherwise, it is defined as $R_{\text{Road}} = 1 - \frac{\text{dis}}{40}$. This incentivizes the model to generate predictions that are geographically aligned with the road network.

$$R_{\text{Road}} = \begin{cases} 1 - \frac{\text{dis}}{40}, & \text{if } \text{dis} \leq 40 \\ 0, & \text{otherwise} \end{cases} \quad (5)$$

Format Reward. In reinforcement learning-based fine-tuning of large language models, it is common to include a Format Reward to ensure structured outputs. In our setting, we require the model to wrap its reasoning process within `< think >` tags and the final answer within `< answer >` tags to facilitate downstream parsing. Additionally, the answer must be a coordinate tuple for further processing. The reward is defined as follows: if the reasoning and answer are properly enclosed in the correct tags, the model receives a reward of 1; if the answer is also correctly formatted as a tuple, the reward is increased to 2. If neither condition is met, the reward is 0. This structured output facilitates both

Table 1: **Comparison Results.** We compare our method with six baselines across all datasets. Our approach consistently achieves SOTA results. The bolded scores indicate the best performance, and the underlined scores indicate the second-best.

	Chengdu		Porto		Sanfrancisco		Rome	
	MAE	RMSE	MAE	RMSE	MAE	RMSE	MAE	RMSE
Small Models								
DeepMove	65.71	53.90	92.65	73.03	91.68	73.43	92.33	75.67
GETNext	71.65	58.27	94.08	74.45	100.24	80.02	97.93	80.02
TrajGDM	101.58	80.30	113.99	90.01	114.87	89.35	128.78	103.08
UniMob	61.96	50.80	113.42	89.63	88.97	72.60	83.46	68.52
Large Language Model-Based								
AgentMove	133.93	108.88	138.60	110.44	169.28	135.96	163.63	131.03
NextLocLLM	89.19	69.13	84.62	67.33	88.60	71.79	83.83	72.40
Vision-Language Model-Based								
VLMLocPredictor	56.81	46.74	83.55	65.88	83.12	69.57	82.53	68.37

interpretability and automated evaluation.

$$R_{\text{Format}} = \begin{cases} 2, & \text{if properly enclosed and correctly formatted} \\ 1, & \text{if the output is properly enclosed} \\ 0, & \text{otherwise} \end{cases} \quad (6)$$

Step Reward. To further encourage structured reasoning, we introduce a Step Reward that rewards multi-step logical thinking. Specifically, we require the model to generate a step-by-step reasoning trace. If the model outputs three or more clearly distinguishable reasoning steps, the reward is 1. Otherwise, it is linearly decayed based on the number of steps using the formula $R_{\text{Step}} = 1 - \frac{3 - \text{step}}{3}$. This reward guides the model toward producing more deliberate, interpretable, and robust reasoning processes.

$$R_{\text{Step}} = \begin{cases} 1, & \text{if steps} \geq 3 \\ 1 - \frac{3 - \text{step}}{3}, & \text{otherwise} \end{cases} \quad (7)$$

Together, these four reward signals serve complementary purposes: Distance1 and Road Rewards guide geographical correctness, Format Reward ensures output quality and structure, and Step Reward promotes transparent and multi-step reasoning. By integrating them within a GRPO-based framework, we efficiently enhance the model’s ability to reason about and predict the next-gps-location on real-world maps.

Experiments

Experimental Settings

Datasets. To evaluate our model’s reasoning ability over visual maps, we construct four visual map-based next-location prediction datasets: Porto, San Francisco, Rome, and Chengdu. Each dataset contains real-world urban trajectories projected onto static map images. We split the data into training, validation, and test sets with a 7:1:2 ratio and conduct comprehensive evaluations on all four cities. Due to

space limitations, detailed descriptions of each dataset can be found in the Appendix.

Evaluation Metrics. We adopt two widely-used metrics for spatial prediction: Mean Average Error(MAE) and Rooted Mean Square Error(RMSE). It worths mentioning that the calculation of MAE and RMSE is slightly different from convention. The MAE calculates the mean average error of the Manhattan distance, and the RMSE calculates the mean average error of the Euclidean distance. The definition can be found in the appendix.

Implementation Details. We use Qwen2-VL-2B as our base model. Our implementation builds upon Open-R1 and Reason-RFT, and inference is accelerated using vLLM. All experiments are conducted on four NVIDIA A100 GPUs (80GB each). We do not report results on larger-scale models such as Qwen2.5-VL-3B due to hardware limitations, as reinforcement learning training is only feasible up to the 2B model size on our infrastructure.

Baselines. We compare our method against six representative and state-of-the-art baselines, including four deep learning models and two large language model (LLM)-based approaches: **RNN**(Elman 1990): A standard recurrent neural network for sequential trajectory modeling. **DeepMove**(Feng et al. 2018): A RNN-transformer hybrid model that captures temporal and spatial patterns in urban mobility. **UniMob**(Long, Yuan, and Li 2025): A unified attention-based architecture for trajectory-based prediction tasks. **TrajGDM**(Chu, Zhang, and Lu 2023): A graph-based diffusion model that models spatiotemporal dependencies via dynamic graph structures. **AgentMove**(Feng et al. 2025): A recent training-free agent-centric model that simulates goal-driven movement in complex urban environments. **NextLocLLM**(Liu et al. 2024): A method that fine-tune a LLM to incorporate POI and GPS information for trajectory prediction.

Comparison Experimental Results

We compare our method with six baseline approaches across all datasets. As shown Table 1, our proposed method consistently achieves state-of-the-art (SOTA) performance, demonstrating its effectiveness. From detailed analysis, we derive the following insights:

1. Classical non-LLM methods yield results that are comparable to large language model-based methods like NextLocLLM. This may be due to the limited semantic richness in GPS coordinates, where the advantage of large-scale language models diminishes.
2. While AgentMove—a semantic-based method—achieves SOTA performance in next-POI-location tasks, it performs less competitively in the next-GPS-location setting. This may be because GPS-level reasoning requires fine-grained spatial understanding, which benefits more from task-specific training and city-specific knowledge.
3. In contrast, our method introduces visual maps and road topology into the reasoning process. By leveraging the VLM’s visual reasoning ability over road networks, our approach achieves SOTA results on most metrics, confirming that incorporating road connectivity leads to more accurate next-GPS-location prediction.

Cross-city Experimental Results

Table 2: **Cross-city Experimental Results Results.** We compare our method with LLM-based approaches under cross-city transfer scenarios.

Target City	Chengdu		Porto	
Source City	MAE	RMSE	MAE	RMSE
AgentMove				
/	133.93	108.88	138.60	110.44
NextLocLLM				
Chengdu	89.01	64.99	150.90	122.99
Porto	87.10	69.03	84.62	67.33
Rome	89.19	69.13	138.07	110.11
Sanfrancisco	92.88	72.44	145.95	117.91
VLMLocPredictor				
Chengdu	56.81	46.74	136.28	109.33
Porto	86.39	68.09	83.55	65.88
Rome	69.21	57.18	131.15	104.55
Sanfrancisco	71.18	58.08	102.99	81.99

Given that LLM-based methods rely heavily on semantic representations, they are often expected to generalize across cities. We evaluate cross-city generalization by comparing our method with AgentMove and NextLocLLM in transfer settings. Specifically, we train models on Chengdu and Porto, then test their performance when transferred to other cities. As shown in Table 2, the results demonstrate that our method achieves superior transferability across urban contexts. Possible reasons include: 1. Although AgentMove is training-free, allowing it to generalize to some extent, its reliance on semantic patterns makes it less effective

in GPS reasoning tasks where explicit spatial cues are sparse. 2. Our method, on the other hand, reasons over road networks using visual maps, which more closely resembles how humans navigate and generalize across unfamiliar environments. This road-aware reasoning likely underpins its consistently better generalization performance.

Ablation Study

To thoroughly validate the effectiveness of our approach, we perform a series of ablation studies on different modules within our framework. In particular, we focus on assessing the contribution of each component and the impact of our reinforcement learning strategy, especially the proposed Road Reward.

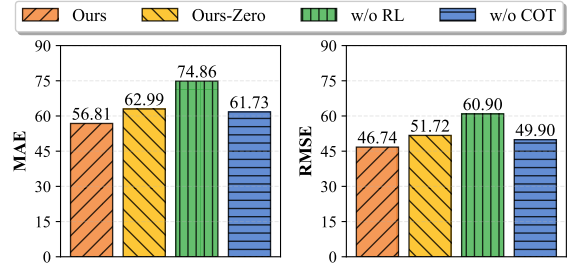


Figure 4: **Ablations on Main Modules.** The left and right figure illustrates the MAE and RMSE of each method.

Ablations on Main Modules We first conduct ablation experiments on the Chengdu dataset to assess the importance of different modules. The experimental settings include: **Ours**: The full VLMLocPredictor model. **Ours-Zero**: Reinforcement learning applied directly to the base model without SFT. **w/o RL**: Only the SFT stage is used; no reinforcement learning is applied. **w/o COT**: During the SFT stage, only the first subtask (coordinate grounding) is used; the second task is removed.

As shown in Figure 4, the results lead to the following conclusions: 1. Our full model consistently achieves the best MAE and RMSE, validating the effectiveness of each component in the framework. 2. Interestingly, Ours-Zero also produces competitive results, suggesting that reinforcement learning enables the model to autonomously learn map-based trajectory reasoning, even without explicit supervision. 3. Although w/o SFT and w/o CF cause only a slight performance drop numerically, qualitative analysis shows that the model’s reasoning outputs become incoherent or nonsensical without these SFT stages. This highlights the necessity of our proposed SFT design, particularly in shaping interpretable thinking processes.

Ablations on Reinforcement Learning To further evaluate the effectiveness of our reinforcement learning design, we conduct additional ablation studies on the Chengdu dataset with a focus on the Road Reward. The settings include: **Ours**: The complete model with full RL and Road Reward. **w/o R.R.**: Road Reward is removed. **w/ e2eSFT**:

Table 3: **Ablations on Reinforcement Learning.** We compare four different settings to demonstrate the effect of RL.

	Chengdu			
	MAE	RMSE	MAERD	RMSERD
Ours	56.81	46.74	10.48	15.62
w/o R.R.	76.70	62.56	11.85	17.20
w/ e2eSFT	96.42	78.12	12.38	18.56
w/ Hard R.R.	71.07	59.72	11.89	16.18

The base model is directly fine-tuned on next-point prediction without reinforcement learning. **w/ Hard R.R.:** The continuous Road Reward is replaced with a binary version: reward is 1 if the predicted point lies on the road network, and 0 otherwise. We also introduce an additional evaluation metric, the Euclidean distance to the nearest road to measure the average distance between the predicted point and the nearest road segment. We use the Mean Average Error(MAE) and Rooted Mean Square Error(RMSE) to evaluate the results. The definition here is the same as the convention. We will show the definition in the Appendix.

As shown in Table 3, the Key findings include: 1. Models trained with reinforcement learning outperform SFT-only baselines, suggesting that RL offers better scalability and learning potential. 2. Incorporating the Road Reward significantly improves prediction accuracy, indicating that our design successfully encourages road-conformant reasoning. 3. The use of our soft reward function, which decays smoothly with distance from the road, outperforms the hard (0-1) reward. This suggests that a continuous reward signal provides a more stable and informative optimization objective for the model.

Case Study on Predicted Points

To further verify the effectiveness and interpretability of our proposed method, we visualize the prediction results of various models on the Chengdu dataset. As shown in Figure 5, we present two representative scenarios.

In the upper part of the figure, we illustrate a trajectory that clearly follows a main road. And the findings are: 1. Our method accurately predicts the next location point, and the prediction lies naturally along the road network, forming a smooth extension of the existing trajectory. This demonstrates the spatial plausibility and effectiveness of our approach. 2. In contrast, nearly all baseline methods fail to produce predictions that align with the road network. This is likely because they rely solely on raw GPS coordinates and lack access to explicit visual or topological map information. 3. Furthermore, our model’s generated reasoning text includes accurate directional cues (e.g., *from the eastern, generally westward*) and spatial descriptions (e.g., *winding path*), showcasing the interpretability of our model’s predictions.

In the lower part of the figure, we present a more challenging case where the next movement requires a turn, where proceeding forward is no longer possible, and at least one

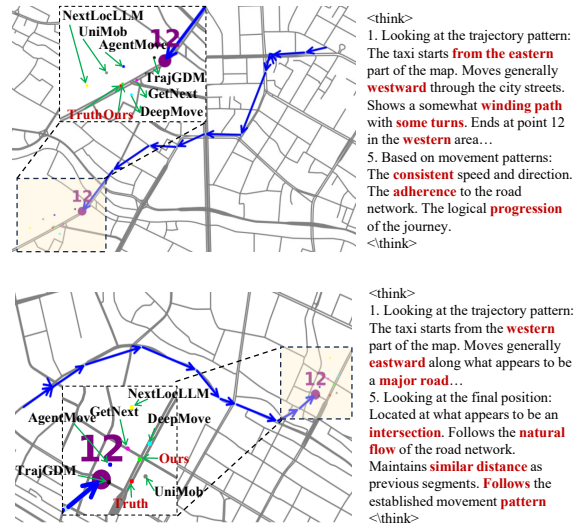


Figure 5: **Case study on predicted points.** The figure showcases two different scenarios to illustrate model behavior.

turn is required—possibly two, depending on the intended path. The findings on this case are: 1. Most baseline models fail to predict this two-turn maneuver, likely due to the lack of explicit map understanding. 2. Our method successfully predicts two sequential turns and outputs a plausible next location, reflecting the precision of our spatial reasoning capability. 3. The reasoning text generated by our model also correctly identifies that the current point is at an *intersection*, and recommends to *follow the natural flow*, again supporting the explainability of our approach.

Case Study on Attention Weight

To further demonstrate that our model is truly capable of reasoning over visual maps, we visualize the attention weights corresponding to the 20th layer of the VLM alongside the generated text, as shown in Figure 6. In the visualizations, green regions indicate high attention weights, while red regions indicate lower attention. The accompanying text represents the model’s generated output, and each attention heatmap corresponds to the token immediately preceding the highlighted word in red.

Our observations are as follows: 1. When the model states “Consider the road network around point 12”, the attention map shows a clear focus around point 12, indicating that the model is referencing the correct spatial region during reasoning. 2. When saying “The last few arrows show a slight curve to northeast”, the attention shifts to the upper-left area, which aligns with the trajectory’s visual curvature. 3. While predicting point 13, the model places higher attention along the trajectory path, whereas irrelevant regions such as the upper-right corner receive minimal attention. 4. When mentioning “start from the western”, the model’s attention is concentrated on the left side of the image, corresponding to the starting point of the trajectory.

These examples demonstrate that, under our proposed

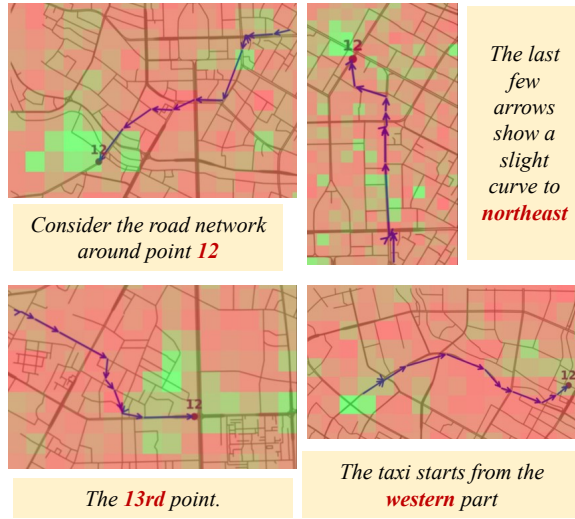


Figure 6: **Case study on Attention Weight.** The cases clearly shows our model is truly capable of reasoning over visual maps.

framework, the model learns to align language with visual context, using the map for token-level spatial reasoning. The attention distributions confirm that the VLM is not generating text arbitrarily, but rather grounding its reasoning process in the visual structure of the map, ultimately leading to more accurate predictions.

Related Work

Next Location Prediction

Next Location Prediction plays a vital role in spatio-temporal modeling, with broad applications in traffic resource optimization, epidemic forecasting, and urban mobility management. This problem can be broadly categorized into two sub-tasks: Next-POI-location prediction, where the goal is to predict the next point-of-interest (POI) the user will visit. Next-GPS-location prediction, where the model aims to predict the exact coordinates of the next point along a trajectory. While the former benefits from the rich semantic context of POIs and can be effectively tackled using large language models (LLMs), the latter poses unique challenges: it contains less semantic information but exhibits strong sequential and geometric patterns. Consequently, this paper focuses on the task of next-GPS-location prediction for taxi trajectories.

Early approaches modeled human mobility using Markov chains(Norris 1998), which capture first-order dependencies but fail to account for longer-term sequential patterns(Gao et al. 2019; Wang et al. 2021). With the rise of deep learning, Recurrent Neural Networks(RNNs) (Elman 1990) and Transformers (Vaswani et al. 2017) were widely adopted for trajectory prediction tasks, yielding promising results(Chen et al. 2023; Feng et al. 2022, 2018). Later, graph-based methods and geographic feature embeddings were introduced to incorporate road network structures and spatial relation-

ships(Long, Yuan, and Li 2025; Yang, Liu, and Zhao 2022). Recently, LLM-based approaches such as LLM-Mob (Wang et al. 2023), Agent-Move (Feng et al. 2025) and NextLo-LLM (Liu et al. 2024) have been proposed to leverage textual and semantic knowledge for mobility prediction. However, these works primarily focus on next-POI-location prediction, where semantic context plays a central role. In contrast, how to effectively model and predict the next GPS coordinate remains an open challenge.

Vision-Language Model

Vision-Language Models (VLMs) are designed to jointly process and reason over textual and visual inputs. Recent advancements have significantly expanded their capabilities, enabling applications in image captioning, visual question answering, and multi-modal instruction following.

VLMs can be broadly categorized into two paradigms based on their learning objectives: **Contrastive Models** that do not support text generation conditioned on visual inputs such as CLIP (Radford et al. 2021) and GLIP (Li et al. 2022). **Generative Models** that incorporating generative architectures, enabling generation across images and text. Examples include the GPT-4 series (OpenAI 2024b,a), Gemini series (Gemini Team 2024b,a), Pixtral (Agrawal et al. 2024; MistralAI 2024), and Claude series (Claude 2024a,b; Anthropic 2023). These models are trained to produce coherent, context-aware outputs conditioned on both images and text, and they have demonstrated impressive performance in tasks requiring complex spatial, temporal, and commonsense reasoning. In this work, we focus specifically on generative VLMs, leveraging their ability to model intricate spatial trajectories over visual maps.

Reinforcement Learning from Verifiable Reward

Recently, Reinforcement Learning from Verifiable Reward (RLVR) has emerged as a key technique for enhancing large language models (LLMs). Beginning with the success of GPT-o1(OpenAI 2024c), researchers have shown that allowing models to self-improve through interaction and feedback from the environment leads to substantial performance gains. This insight gave rise to models like DeepSeek-R1(Guo et al. 2025), Gemini-Flash-Thinking(Gemini Team 2024b), and Claude4(Claude 2025), all of which employ RLVR to refine model behaviors. The core RLVR techniques typically build upon policy optimization frameworks such as PPO(Schulman et al. 2017) and DPO(Rafailov et al. 2023), while recent works like DeepSeek-R1 adopt GRPO(Shao et al. 2024), a lightweight alternative that optimizes relative advantages without relying on value networks.

However, only recently have researchers begun to explore RL-based post-training in the visual modality. Pioneering works such as GPT-o3(OpenAI 2025), Visual-RFT(Liu et al. 2025), and Reason-RFT(Tan et al. 2025) demonstrate promising early results, extending reinforcement learning techniques to vision-language settings. Despite this progress, a key question remains underexplored: How can reinforcement learning be applied to enhance VLMs' ability to perform spatial reasoning, specifically in the context of next-location prediction?

Conclusion

In this work, we explore the use of Vision-Language Models (VLMs) for next-GPS-location prediction. We first propose a method called Vision-Guided Location Search (VGLS) to assess the inherent next-GPS-location reasoning capabilities of VLMs without modifying their internal parameters. Our findings reveal that while larger models exhibit implicit reasoning ability—even without the capacity to explicitly output coordinates—smaller models generally lack such capabilities. To explicitly equip VLMs with next-GPS-location prediction ability, we introduce a two-stage training framework. Experiments on four urban datasets demonstrate that our approach achieves state-of-the-art results. Looking ahead, future work may explore training on larger-scale and more diverse datasets, with the goal of building a model that consistently outperforms non-LLM baselines across a wide range of cities.

References

- Abacha, A. B.; wai Yim, W.; Fu, Y.; Sun, Z.; Yetisgen, M.; Xia, F.; and Lin, T. 2025. MEDEC: A Benchmark for Medical Error Detection and Correction in Clinical Notes. arXiv:2412.19260.
- Agrawal, P.; Antoniak, S.; Hanna, E. B.; Bout, B.; Chaplot, D.; Chudnovsky, J.; Costa, D.; Monicault, B. D.; Garg, S.; Gervet, T.; Ghosh, S.; Héliou, A.; Jacob, P.; Jiang, A. Q.; Khandelwal, K.; Lacroix, T.; Lample, G.; Casas, D. L.; Lavril, T.; Scao, T. L.; Lo, A.; Marshall, W.; Martin, L.; Mensch, A.; Muddireddy, P.; Nemychnikova, V.; Pellat, M.; Platen, P. V.; Raghuraman, N.; Rozière, B.; Sablayrolles, A.; Saulnier, L.; Sauvestre, R.; Shang, W.; Soletskyi, R.; Stewart, L.; Stock, P.; Studnia, J.; Subramanian, S.; Vaze, S.; Wang, T.; and Yang, S. 2024. Pixtral 12B. arXiv:2410.07073.
- Anthropic. 2023. Claude-2.1. Accessed: 2025-01-20.
- Cabanas-Tirapu, O.; Danús, L.; Moro, E.; Sales-Pardo, M.; and Guimerà, R. 2023. Human mobility is well described by closed-form gravity-like models learned automatically from data. *CoRR*, abs/2312.11281.
- Chen, Y.; Xu, H.; Chen, X. M.; and Gao, Z. 2023. A multi-scale unified model of human mobility in urban agglomerations. *Patterns*, 4(11): 100862.
- Chu, C.; Zhang, H.; and Lu, F. 2023. TrajGDM: A New Trajectory Foundation Model for Simulating Human Mobility. In Renz, M.; and Nascimento, M. A., eds., *Proceedings of the 31st ACM International Conference on Advances in Geographic Information Systems, SIGSPATIAL 2023, Hamburg, Germany, November 13-16, 2023*, 1:1–1:2. ACM.
- Claude. 2024a. Claude 3 Haiku: our fastest model yet.
- Claude. 2024b. Claude 3.5 Sonnet.
- Claude. 2025. Introducing Claude 4.
- Elman, J. L. 1990. Finding Structure in Time. *Cogn. Sci.*, 14(2): 179–211.
- Fang, S.; Zhang, Q.; Meng, G.; Xiang, S.; and Pan, C. 2019. GSTNet: Global Spatial-Temporal Network for Traffic Flow Prediction. In Kraus, S., ed., *Proceedings of the Twenty-Eighth International Joint Conference on Artificial Intelligence, IJCAI 2019, Macao, China, August 10-16, 2019*, 2286–2293. ijcai.org.
- Feng, J.; Du, Y.; Zhao, J.; and Li, Y. 2025. AgentMove: A Large Language Model based Agentic Framework for Zero-shot Next Location Prediction. In Chiruzzo, L.; Ritter, A.; and Wang, L., eds., *Proceedings of the 2025 Conference of the Nations of the Americas Chapter of the Association for Computational Linguistics: Human Language Technologies, NAACL 2025 - Volume 1: Long Papers, Albuquerque, New Mexico, USA, April 29 - May 4, 2025*, 1322–1338. Association for Computational Linguistics.
- Feng, J.; Li, Y.; Lin, Z.; Rong, C.; Sun, F.; Guo, D.; and Jin, D. 2022. Context-aware Spatial-Temporal Neural Network for Citywide Crowd Flow Prediction via Modeling Long-range Spatial Dependency. *ACM Trans. Knowl. Discov. Data*, 16(3): 49:1–49:21.

- Feng, J.; Li, Y.; Zhang, C.; Sun, F.; Meng, F.; Guo, A.; and Jin, D. 2018. DeepMove: Predicting Human Mobility with Attentional Recurrent Networks. In Champin, P.; Gandon, F.; Lalmas, M.; and Ipeirotis, P. G., eds., *Proceedings of the 2018 World Wide Web Conference on World Wide Web, WWW 2018, Lyon, France, April 23-27, 2018*, 1459–1468. ACM.
- Gao, Q.; Zhou, F.; Trajcevski, G.; Zhang, K.; Zhong, T.; and Zhang, F. 2019. Predicting Human Mobility via Variational Attention. In Liu, L.; White, R. W.; Mantrach, A.; Silvestri, F.; McAuley, J. J.; Baeza-Yates, R.; and Zia, L., eds., *The World Wide Web Conference, WWW 2019, San Francisco, CA, USA, May 13-17, 2019*, 2750–2756. ACM.
- Gemini Team, G. 2024a. Gemini 1.5: Unlocking multimodal understanding across millions of tokens of context.
- Gemini Team, G. 2024b. Gemini 2.0 Flash Thinking Experimental.
- Guo, D.; Yang, D.; Zhang, H.; Song, J.; Zhang, R.; Xu, R.; Zhu, Q.; Ma, S.; Wang, P.; Bi, X.; et al. 2025. Deepseek-r1: Incentivizing reasoning capability in llms via reinforcement learning. *arXiv preprint arXiv:2501.12948*.
- Li, L. H.; Zhang, P.; Zhang, H.; Yang, J.; Li, C.; Zhong, Y.; Wang, L.; Yuan, L.; Zhang, L.; Hwang, J.; Chang, K.; and Gao, J. 2022. Grounded Language-Image Pre-training. In *IEEE/CVF Conference on Computer Vision and Pattern Recognition, CVPR 2022, New Orleans, LA, USA, June 18-24, 2022*, 10955–10965. IEEE.
- Liu, S.; Cao, N.; Chen, Y.; Jiang, Y.; and Cong, G. 2024. nextlocllm: next location prediction using LLMs. *CoRR*, abs/2410.09129.
- Liu, Z.; Sun, Z.; Zang, Y.; Dong, X.; Cao, Y.; Duan, H.; Lin, D.; and Wang, J. 2025. Visual-rft: Visual reinforcement fine-tuning. *arXiv preprint arXiv:2503.01785*.
- Llama, M. 2024. Llama 3.2: Revolutionizing edge AI and vision with open, customizable models.
- Long, Q.; Yuan, Y.; and Li, Y. 2025. A Universal Model for Human Mobility Prediction. In Sun, Y.; Chierichetti, F.; Lauw, H. W.; Perlich, C.; Tok, W. H.; and Tomkins, A., eds., *Proceedings of the 31st ACM SIGKDD Conference on Knowledge Discovery and Data Mining, V.1, KDD 2025, Toronto, ON, Canada, August 3-7, 2025*, 894–905. ACM.
- Mayemba, C. N.; Nkashama, D. K.; Tshimula, J. M.; Dimalufuma, M. V.; Muabila, J. T.; Didier, M. M.; Kanda, H.; Galekwa, R. M.; Fita, H. D.; Mundeke, S.; et al. 2024. A short survey of human mobility prediction in epidemic modeling from transformers to llms. *arXiv preprint arXiv:2404.16921*.
- MistralAI. 2024. Pixtral Large.
- Norris, J. R. 1998. *Markov chains*. 2. Cambridge university press.
- OpenAI. 2024a. GPT-4o mini: advancing cost-efficient intelligence.
- OpenAI. 2024b. Hello GPT-4o.
- OpenAI. 2024c. Learning to reason with LLMs.
- OpenAI. 2025. Introducing OpenAI o3 and o4-mini.
- Pappalardo, L.; Barlacchi, G.; Pellungrini, R.; and Simini, F. 2019. Human Mobility from theory to practice: Data, Models and Applications. In Amer-Yahia, S.; Mahdian, M.; Goel, A.; Houben, G.; Lerman, K.; McAuley, J. J.; Baeza-Yates, R.; and Zia, L., eds., *Companion of The 2019 World Wide Web Conference, WWW 2019, San Francisco, CA, USA, May 13-17, 2019*, 1311–1312. ACM.
- Radford, A.; Kim, J. W.; Hallacy, C.; Ramesh, A.; Goh, G.; Agarwal, S.; Sastry, G.; Askell, A.; Mishkin, P.; Clark, J.; Krueger, G.; and Sutskever, I. 2021. Learning Transferable Visual Models From Natural Language Supervision. In Meila, M.; and Zhang, T., eds., *Proceedings of the 38th International Conference on Machine Learning, ICML 2021, 18-24 July 2021, Virtual Event*, volume 139 of *Proceedings of Machine Learning Research*, 8748–8763. PMLR.
- Rafailov, R.; Sharma, A.; Mitchell, E.; Manning, C. D.; Ermon, S.; and Finn, C. 2023. Direct Preference Optimization: Your Language Model is Secretly a Reward Model. In Oh, A.; Naumann, T.; Globerson, A.; Saenko, K.; Hardt, M.; and Levine, S., eds., *Advances in Neural Information Processing Systems 36: Annual Conference on Neural Information Processing Systems 2023, NeurIPS 2023, New Orleans, LA, USA, December 10 - 16, 2023*.
- Schulman, J.; Wolski, F.; Dhariwal, P.; Radford, A.; and Klimov, O. 2017. Proximal policy optimization algorithms. *arXiv preprint arXiv:1707.06347*.
- Shao, Z.; Wang, P.; Zhu, Q.; Xu, R.; Song, J.; Bi, X.; Zhang, H.; Zhang, M.; Li, Y.; Wu, Y.; et al. 2024. Deepseekmath: Pushing the limits of mathematical reasoning in open language models. *arXiv preprint arXiv:2402.03300*.
- Shtedritski, A.; Rupprecht, C.; and Vedaldi, A. 2023. What does CLIP know about a red circle? Visual prompt engineering for VLMs. In *IEEE/CVF International Conference on Computer Vision, ICCV 2023, Paris, France, October 1-6, 2023*, 11953–11963. IEEE.
- Song, C.; Qu, Z.; Blumm, N.; and Barabási, A.-L. 2010. Limits of predictability in human mobility. *Science*, 327(5968): 1018–1021.
- Tan, H.; Ji, Y.; Hao, X.; Lin, M.; Wang, P.; Wang, Z.; and Zhang, S. 2025. Reason-rft: Reinforcement fine-tuning for visual reasoning. *arXiv preprint arXiv:2503.20752*.
- Team, Q. 2024. QVQ: To See the World with Wisdom.
- Vaswani, A.; Shazeer, N.; Parmar, N.; Uszkoreit, J.; Jones, L.; Gomez, A. N.; Kaiser, L.; and Polosukhin, I. 2017. Attention is All you Need. In Guyon, I.; von Luxburg, U.; Bengio, S.; Wallach, H. M.; Fergus, R.; Vishwanathan, S. V. N.; and Garnett, R., eds., *Advances in Neural Information Processing Systems 30: Annual Conference on Neural Information Processing Systems 2017, December 4-9, 2017, Long Beach, CA, USA*, 5998–6008.
- Wang, H.; Li, Y.; Jin, D.; and Han, Z. 2021. Attentional Markov Model for Human Mobility Prediction. *IEEE J. Sel. Areas Commun.*, 39(7): 2213–2225.
- Wang, J.; Kong, X.; Xia, F.; and Sun, L. 2019. Urban Human Mobility: Data-Driven Modeling and Prediction. *SIGKDD Explor.*, 21(1): 1–19.

Wang, P.; Bai, S.; Tan, S.; Wang, S.; Fan, Z.; Bai, J.; Chen, K.; Liu, X.; Wang, J.; Ge, W.; Fan, Y.; Dang, K.; Du, M.; Ren, X.; Men, R.; Liu, D.; Zhou, C.; Zhou, J.; and Lin, J. 2024. Qwen2-VL: Enhancing Vision-Language Model’s Perception of the World at Any Resolution. *arXiv preprint arXiv:2409.12191*.

Wang, X.; Fang, M.; Zeng, Z.; and Cheng, T. 2023. Where Would I Go Next? Large Language Models as Human Mobility Predictors. *CoRR*, abs/2308.15197.

Wu, P.; and Xie, S. 2024. V*: Guided Visual Search as a Core Mechanism in Multimodal LLMs. In *IEEE/CVF Conference on Computer Vision and Pattern Recognition, CVPR 2024, Seattle, WA, USA, June 16-22, 2024*, 13084–13094. IEEE.

Yang, S.; Liu, J.; and Zhao, K. 2022. GETNext: Trajectory Flow Map Enhanced Transformer for Next POI Recommendation. In Amigó, E.; Castells, P.; Gonzalo, J.; Carterette, B.; Culpepper, J. S.; and Kazai, G., eds., *SIGIR ’22: The 45th International ACM SIGIR Conference on Research and Development in Information Retrieval, Madrid, Spain, July 11 - 15, 2022*, 1144–1153. ACM.

Zhang, C.; and Patras, P. 2018. Long-Term Mobile Traffic Forecasting Using Deep Spatio-Temporal Neural Networks. In *Proceedings of the Nineteenth ACM International Symposium on Mobile Ad Hoc Networking and Computing, MobiHoc 2018, Los Angeles, CA, USA, June 26-29, 2018*, 231–240. ACM.

Zhang, J.; Yang, Y.; Wu, X.; and Li, S. 2025a. Spatio-temporal transformer and graph convolutional networks based traffic flow prediction. *Scientific Reports*, 15(1): 24299.

Zhang, R.; Tai, J.; Yao, Q.; Yang, W.; Ruggeri, K.; Shaman, J.; and Pei, S. 2025b. Behavior-driven forecasts of neighborhood-level COVID-19 spread in New York City. *PLOS Computational Biology*, 21(4): e1012979.

Zhao, B.; Wang, X.; Zhang, T.; Shi, R.; Xu, F.; Man, F.; Chen, E.; Li, Y.; Li, Y.; Sun, T.; et al. 2024. Estimating and modeling spontaneous mobility changes during the COVID-19 pandemic without stay-at-home orders. *Humanities and Social Sciences Communications*, 11(1): 1–15.

Appendix

The Predictability of Next Location

While the next location inherently involves some degree of randomness, one might question whether it is truly predictable.

However, from an intuitive standpoint, the next location is far from arbitrary. In the context of urban mobility, especially in taxi trajectories, drivers often follow near-optimal routes constrained by the road network and influenced by practical factors such as traffic flow and passenger destinations. Crucially, these constraints and patterns are often reflected in the driver’s past trajectory, including route choice, directionality, and speed. As a result, the feasible space for the next point is significantly narrowed, making the next location partially deterministic and thus predictable to a meaningful extent.

This intuition is supported by empirical findings. For example, (Song et al. 2010) demonstrates—through rigorous mathematical analysis—that human mobility, as captured by signaling data, exhibits a predictability upper bound of nearly 70%. This confirms that the movement patterns contain strong patterns.

Moreover, even if the next location cannot be predicted with perfect accuracy, the task remains valuable and well-founded. It shares similarities with next-token prediction in language modeling, where multiple plausible continuations exist, yet predictive modeling has led to breakthroughs in understanding and generation. By analogy, next-location prediction can be framed as a probabilistic and context-aware spatial reasoning task, making it a meaningful and well-posed challenge.

Experimental Settings of the Preliminary Experiment

In this section, we introduce additional experimental settings of the **preliminary task**. Generally, the preliminary task using the same chengdu dataset as the main experiment. We only report the baselines and additional experimental settings in the preliminary experiment here.

Experimental Settings. Most vision-language models were accessed via the OpenRouter API¹. Especially, GeminiFlash2 Thinking was accessed through Google AI Studio².

Calculation of MAE and RMSE in Comparison Experiment To evaluate the performance of our next GPS location prediction model, we use two widely adapted distance-based metrics: **Mean Absolute Error (MAE)** and **Root Mean Squared Error (RMSE)**. Different from conventional design, we redefined the calculation for coordinate-level trajectory tasks as follows:

Mean Absolute Error (MAE). Given a predicted point $\hat{p}_i = (\hat{x}_i, \hat{y}_i)$ and the ground-truth point $p_i = (x_i, y_i)$, the MAE is computed as the average Manhattan distance be-

¹<https://openrouter.ai>

²<https://aistudio.google.com/>

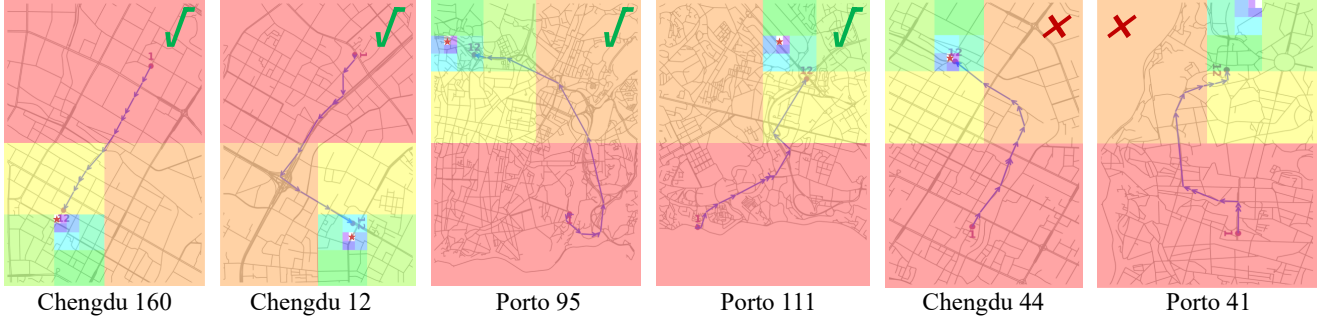


Figure 7: **Case Study of the Preliminary Experiment.** The examples are all taken from the predictions of Claude3.5 Sonet. The first four represent reasonable predictions, while the last two correspond to less reasonable predictions. The colored regions indicate areas that the model has excluded from consideration, and the red star marks the model’s final predicted location.

tween the predicted and actual coordinates:

$$\text{MAE} = \frac{1}{N} \sum_{i=1}^N (|\hat{x}_i - x_i| + |\hat{y}_i - y_i|) \quad (8)$$

Root Mean Squared Error (RMSE). The RMSE is defined as the mean error of the Euclidean distance between the predicted and true locations:

$$\text{RMSE} = \frac{1}{N} \sum_{i=1}^N \left(\sqrt{(\hat{x}_i - x_i)^2 + (\hat{y}_i - y_i)^2} \right) \quad (9)$$

where N is the number of evaluated trajectory points.

Calculation of MAE and RMSE in Evaluating Road Reward To evaluate the performance of the Road Reward prediction model, we use two widely adapted distance-based metrics: **Mean Absolute Error (MAE)** and **Root Mean Squared Error (RMSE)**. However, the MAE and RMSE here follow the conventional design:

Mean Absolute Error (MAE). MAE measures the average absolute Euclidean distance between predicted and ground-truth coordinates. It is defined as:

$$\text{MAE} = \frac{1}{N} \sum_{i=1}^N \left(\sqrt{(\hat{x}_i - x_i)^2 + (\hat{y}_i - y_i)^2} \right) \quad (10)$$

Root Mean Squared Error (RMSE). RMSE emphasizes larger errors by squaring the differences before averaging. It is defined as:

$$\text{RMSE} = \sqrt{\frac{1}{N} \sum_{i=1}^N \left\| \sqrt{(\hat{x}_i - x_i)^2 + (\hat{y}_i - y_i)^2} \right\|^2} \quad (11)$$

Baselines. In the preliminary experiment, we only compare with general VLMs: including Gemini-Flash2 Thinking 1219(Gemini Team 2024b)(Guessed to be $\sim 175\text{B}$), and QVQ-72B-Preview(Team 2024),

Claude3.5-Sonet($\sim 175\text{B}$)(Claude 2024b), Claude3-Haiku(Guessed to be $\sim 8\text{B}$)(Claude 2024a), Qwen2VL-72B-Instruct(Wang et al. 2024), Qwen2VL-7B-Instruct, Qwen2VL-2B-Instruct(Wang et al. 2024), Pixtral-Large-2411(124B)(MistralAI 2024), Pixtral-12B(Agrawal et al. 2024), GPT4o($\sim 200\text{B}$)(OpenAI 2024b), GPT4o-mini($\sim 8\text{B}$)(OpenAI 2024a), Llama3.2-90B-vision-Instruct(Llama 2024), and Llama3.2-11B-vision-Instruct(Llama 2024). The number of parameters of some models are derived from (Abacha et al. 2025). The *Instruct* in model name may be omitted for simplicity. Because GPT-o1(OpenAI 2024c) temporarily only supports their tier-5 users, we did not compare with it.

Case Study of the Preliminary Experiment

In this section, we present a visual analysis of selected prediction results from Claude 3.5 Sonet. The first four examples illustrate reasonable predictions, while the last two exhibit less reasonable outcomes.

First, in the Chengdu160 trajectory, which features near-uniform motion, the model accurately predicts the next location along the uniform trajectory, demonstrating its inherent spatial reasoning capabilities. Similarly, in the Chengdu12 trajectory, the model successfully identifies a feasible turning point after a curve, suggesting that it has learned a reasonable understanding of the topological relationships within the road network. In more complex scenarios, such as Porto95 and Porto111, the model effectively selects a viable next location based on both the trajectory and road network constraints, further supporting its capability for next-location prediction.

However, the model’s predictions can sometimes be influenced by previous trajectory patterns. For instance, in Chengdu44, the movement from the fourth to the fifth point is minimal, leading the model to predict a stop at the 13th point. Conversely, in Porto41, where the displacement between the 6th and 7th points is large, the model overestimates the movement range when predicting the 13th point. While these latter predictions may appear suboptimal, they still indicate that the model is capturing historical trajectory

patterns. This suggests that its predictive capabilities can be further improved with additional refinement and training.

Further Descriptions of Each Dataset

We utilize four publicly available datasets collected from Chengdu, Porto, San Francisco, and Rome. Due to computational constraints, we randomly sample 1,500 trajectories from each dataset and split them into training, validation, and test sets using a 7:1:2 ratio.

In the SFT phase for point localization, we generate 12 question-answer pairs for each trajectory, corresponding to the location of each point on the map. We deliberately avoid prompting the model to predict all 12 points in a single pass. Preliminary experiments showed that requesting all point coordinates at once often led to confusion in the later positions. Therefore, we design each sample to ask the model to predict only one specific point per instance.

In the SFT phase for Chain-of-Thought (CoT) generation, we curate 300 high-quality CoT samples per dataset. These samples are used to train the model’s basic reasoning ability, and some of the examples are shown in later sections.

Prompts

As the Qwen-2-VL has basic object detection ability, and can output object detection result in the format like `< |object_ref_start| > the1thpoint < |object_ref_end| >< |box_start| > (749,500), (750,501) < |box_end| >`, we reuse their ability in our method.

Prompt of VGLS

Hello, you are an expert in next-location prediction.

Known Information:

- 1. This trajectory represents the movement of a taxi driver.
- 2. Each arrow represents the distance and direction of movement over approximately 45 seconds
- 3. The 11 arrows in the diagram show the sequential movement from the first trajectory point to the 12th trajectory point.
- 4. The starting position is marked with a purple dot labeled as point 1 in the diagram, and the current position is marked with a purple dot labeled as point 12.
- 5. Gray lines in the diagram represent drivable roads, while white areas indicate buildings or other obstacles.

Question:

- Based on the following requirements, determine whether the next position (the 13th trajectory point approximately 45 seconds later from the current purple dot position (the 12th trajectory point) is more likely to be in the blue region or the yellow region.

Requirements:

- Return the answer in JSON format, containing a key ANS. If the final answer is the blue region, the value should be 0; if the final answer is the yellow region, the value should be 1.2. Let’s think step by step.

Prompt of Point Localization

You are a trajectory reasoning assistant, and you need to complete the trajectory reasoning task according to the following rules.

Known Information:

- 1. This trajectory represents the movement of a taxi driver.
- 2. Each arrow represents the distance and direction of movement over approximately 45 seconds.
- 3. The 11 arrows in the diagram show the sequential movement from the first trajectory point to the 12th trajectory point.
- 4. The starting position is marked with a purple dot labeled as point 1 in the diagram, and the last position is marked with a purple dot labeled as point 12.
- 5. Gray lines in the diagram represent drivable roads, while white areas indicate buildings or other obstacles.

Requirements:

- 1. Let’s think step by step.
- 2. Output the final answer in `|answer|` tags.
- 3. The final answer should be covered in a `< |box_start| >< |box_end| >` tags. For example, `< |box_start| > (749,500), (750,501) < |box_end| >`.

Questions:

- 1. Based on the following requirements, output the location of the 1th trajectory point. . In the format like `< |object_ref_start| > the1thpoint < |object_ref_end| >< |box_start| > (749,500), (750,501) < |box_end| >`

`< image >`

Prompt of Generating the COT Data

You are a trajectory reasoning assistant, and you need to complete the trajectory reasoning task according to the following rules.

Known Information:

- 1. This trajectory represents the movement of a taxi driver.
- 2. Each arrow represents the distance and direction of movement over approximately 45 seconds.
- 3. The 12 arrows in the diagram show the sequential movement from the first trajectory point to the 12th trajectory point.
- 4. The starting position is marked with a purple dot labeled as point 1 in the diagram, and the last position is marked with a purple dot labeled as point 13.
- 5. Gray lines in the diagram represent drivable roads, while white areas indicate buildings or other obstacles.

Requirements:

- 1. Let's think step by step.
- 2. Output a confidence score between 0 and 1 after your thinking process in json format like "confidence": 0.9.

Questions:

- 1. You should generate a chain-of-thought thinking process to reason the 13th point without mentioning it. And do not conclude, just output reasoning process.
- 2. You should last judge whether the 13th point is the current position of the taxi driver given the first 12 points, output the confidence of your judgment.

Prompt of Predicting the 13rd point

You are a trajectory reasoning assistant, and you need to complete the trajectory reasoning task according to the following rules.

Known Information:

- 1. This trajectory represents the movement of a taxi driver.
- 2. Each arrow represents the distance and direction of movement over approximately 45 seconds.
- 3. The 11 arrows in the diagram show the sequential movement from the first trajectory point to the 12th trajectory point.
- 4. The starting position is marked with a purple dot labeled as point 1 in the diagram, and the last position is marked with a purple dot labeled as point 12.
- 5. Gray lines in the diagram represent drivable roads, while white areas indicate buildings or

other obstacles.

Requirements:

- 1. Let's think step by step.
- 2. Output the final answer in `answer_i` / `answer_i` tags.
- 3. The final answer should be covered in a `<|box_start| ><|box_end| >` tags. For example, `<|box_start| > (749, 500), (750, 501) <|box_end| >`.

Questions:

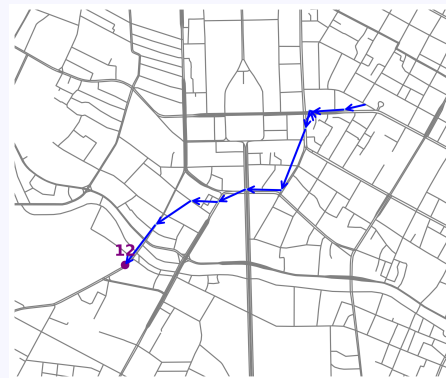
- 1. Based on the following requirements, predict the location of the 13th trajectory point. In the format like `<|object_ref_start| > the13thpoint <|object_ref_end| ><|box_start| > (749, 500), (750, 501) <|box_end| >`

`< image >`

Sample Outputs of VLMLocPredictor

We omit the `<|object_ref_start| >`, `<|object_ref_end| >`, `<|box_start| >`, `<|box_end| >` symbols in the output. In addition, Qwen-2-VL scale the output position to 1000 x 1000, which means the output coordinate need to be rescaled to original position.

Sample1



`< think >`

Let me reason about this step by step:

1. Looking at the trajectory pattern:

- The taxi starts from the eastern part of the map
- Moves generally westward through the city streets
- Shows a somewhat winding path with some turns
- Ends at point 12 in the western area

2. Analyzing the movement characteristics:

- Each arrow represents about 45 seconds of movement

- - The arrows are fairly consistent in length, suggesting relatively constant speed
- - The driver follows the available road network
- - No illegal movements through buildings or obstacles are shown

3. Examining the final movements:

- - The last few arrows (9-12) show a clear westward movement
- - The driver appears to be following a main road
- - The final arrows lead to point 12
- - The movement pattern suggests a typical taxi service behavior

4. Considering the road network around point 12:

- - Point 12 is located at what appears to be an intersection
- - There are multiple possible directions available from this point
- - The previous movement pattern suggests a likely destination rather than a random stop

5. Based on movement patterns:

- - The consistent speed and direction
- - The adherence to the road network
- - The logical progression of the journey
- - The typical behavior of taxi services

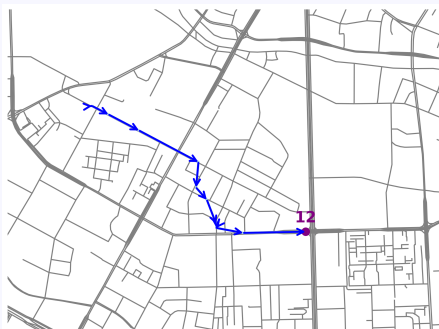
< /think >

< answer >

the 13th point(199,730),(200,731)

< /answer >

Sample2



< think >

Let me reason about this step by step:

1. Looking at the trajectory pattern:

- - The taxi starts from the western part of the map
- - Moves generally eastward along what appears to be a major road

- - The movement is relatively consistent in speed (arrow lengths are similar)
- - The final arrows lead to point 12 in the eastern part of the map

2. Analyzing the movement characteristics:

- - Each arrow represents about 45 seconds of movement
- - The driver maintains a fairly steady speed throughout
- - No sudden turns or speed changes are observed
- - The movement follows the available road network

3. Examining the final segment:

- - The last few arrows (9-12) show a slight curve to the southeast
- - The speed remains consistent
- - The driver appears to be following the main road
- - The final arrows lead to point 12

4. Considering the road network:

- - The area around point 12 shows multiple possible road options
- - The previous movement pattern suggests a preference for main roads
- - The available road network constrains possible movement directions
- - The main road continues in the same general direction

5. Based on movement patterns:

- - The consistent speed and direction suggest a predictable trajectory
- - No erratic movements or unexpected turns
- - The driver appears to be following a planned route
- - The final arrows indicate a natural continuation of the previous movement

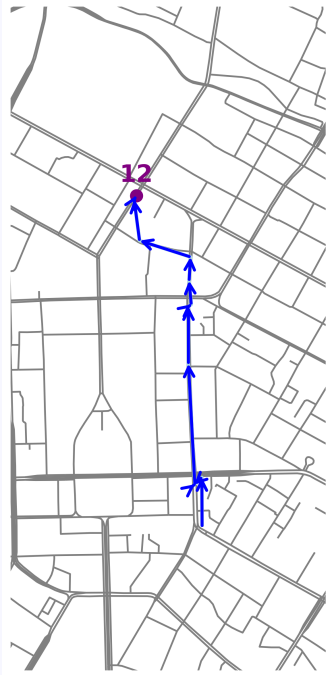
< /think >

< answer >

the 13th point(790,680),(791,681)

< /answer >

Sample3



< think >

Let me reason about this step by step:

1. Looking at the trajectory pattern:

- The taxi starts from the bottom of the map
- Moves generally northward along what appears to be a major road
- The arrows show consistent speed and direction for most segments

2. Analyzing the movement characteristics:

- Each arrow represents about 45 seconds of movement
- The arrows are roughly equal in length, suggesting relatively constant speed
- The driver follows the road network without any sudden turns

3. Examining the final Movements:

- The last few arrows (9-12) show a slight curve to the northeast
- The speed appears consistent throughout
- The driver follows the available road network

4. Considering the road network around point 12:

- There are limited possible directions for the next movement
-
- The previous movement pattern suggests a preference for following the main road

- The available road options are constrained by the road layout

5. Based on movement patterns:

- The consistent speed and direction suggest a predictable trajectory
-
- The driver appears to be following a main arterial route
- The final movements indicate a slight curve rather than a sharp turn

6. Analyzing the final position (point 13):

- Located slightly northeast of point 12
- Follows the available road network
- Maintains similar distance as previous segments
- Follows the natural flow of the previous movement pattern

< /think >

< answer >

the 13th point(380,259),(381,260)

< /answer >